1. Introduction

Dicyclanil (DC), 4,6-diamino-2-cyclopropylamino-pyrimidine-5-carbonitrile, is a pyrimidine-derived insect growth regulator inhibiting the molting and development of insecticides, and is used in a veterinary field for the prevention of myiasis (fly-strike) in sheep. As a result, small amounts of the parent drug and its metabolites are sometimes detected as residues in the edible tissues of these sheep (WHO, 2000). In an 18-month study conducted on the carcinogenicity of DC, it was observed that the incidence of hepatocellular carcinomas was increased in mice fed on a diet containing 1500 ppm of DC; hepatocellular necrosis was also observed in the groups fed with 100 ppm or more of DC (WHO, 2000). On the other hand, in studies conducted on the genotoxicity of DC, negative results were obtained from the in vivo and in vitro tests, and it was evaluated by the 54th meeting of the Joint FAO/WHO Expert Committee on Food Additives (JECFA) that DC is a non-genotoxic carcinogen (WHO, 2000). Additionally, our recent study indicated that negative results were obtained when a single oral administration of DC was performed in the in vivo comet assay using mice and in vivo liver initiation assay using rats, and these results support the evaluation of the JECFA (Moto et al., 2003). Therefore, it was postulated that the DC treatment-induced enhancement of hepatocarcinogenesis resulted from non-genotoxic mechanisms or tumor-promoting actions such as the enhancement of cell proliferation, inhibition of apoptosis, disorder of the cell cycle regulation, secondary genotoxicity, and so on. However, detailed investigations of molecular events in the DC-induced mice liver have not yet been performed.

In the studies conducted to evaluate the mechanism of chemical carcinogenesis, it is extremely important to understand the molecular events during the chemical-induced initiation and promotion phases in the target organs, because gene alterations may vary with the presence or absence of mutated cells and/or preneoplastic foci. Recently, large-scale gene expression analyses by the cDNA microarray have been applied in the fields of toxicology and carcinogenicity (Afshari et al., 1999; Irwin et al., 2004). Microarray analyses have been used to investigate the molecular events in the non-genotoxic carcinogens during the various stages of carcinogenesis, and the molecular events on tumor promoting mechanisms have also been reported (Chen et al., 2001; Iida et al., 2003; Kinoshita et al., 2003; Kato et al., 2004). Several non-genotoxic carcinogens are known to show tumor-promoting activities in the two-stage (initiation-promotion) carcinogenesis models (Shirai, 1997; Shibutani et al., 2002). Therefore, the presently discussed carcinogenesis model is believed to be useful in the detection of molecular profiles during the tumor promotion stage.

In the present study, to clarify the enhancement mechanism of hepatocarcinogenesis in DC-induced mice, a large-scale cDNA microarray (3800 genes) was performed to obtain primary information on molecules and/or molecular events associated with the enhancement of hepatocarcinogenesis in mice liver at the early stage of the toxicity and carcinogenicity of DC. Based on the results obtained from this microarray, a low-density and pathway-specific microarray (112 genes) were performed to investigate the details of the molecular events during the tumor promotion phase of DC using the two-stage hepatocarcinogenesis model in mice with partial hepatectomy. In addition, to clarify the mechanism of the tumor promoting effect of DC, further analyses comprising RT-PCR or real-time RT-PCR, histological examinations, and measurements of proteins associated with the pathway were carried out by taking into account the results obtained from the microarray analyses.

2. Materials and methods

2.1. Animal and experimental design

Four-week-old male ICR mice were purchased from Japan SLC (Japan) and maintained on a powdered basal diet (MF; Oriental Yeast, Japan) and tap water until they were 5-weeks-old; the study was started at this stage. The mice were housed in polycarbonate cages with paper beddings under standard conditions (room temperature, 22 ± 2 °C; relative humidity, 55 ± 5%; light/dark cycle, 12 h).

For the first investigation involving gene expression in the DC-treated liver, the mice were fed on the powdered diet containing DC (Novartis Animal Health, Switzerland) at 0 or 1500 ppm for 2 weeks (Exp. I). On the base of Exp. I, a two-stage liver carcinogenesis model in mice was employed in this study for

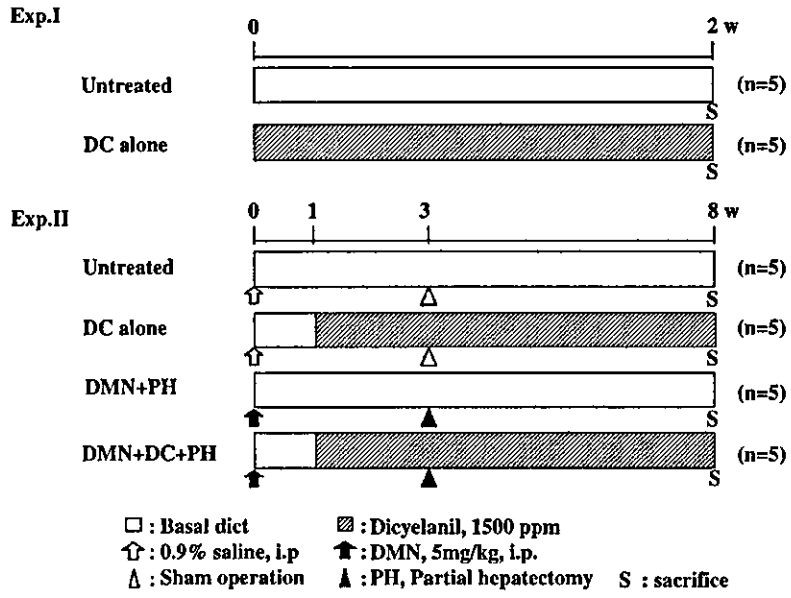

Fig. 1. Experimental designs of Exp. I and II.

the subsequent gene investigations (Fig. 1). To initiate hepatocarcinogenesis, a single i.p. injection of *N*-dimethylnitrosamine (DMN: Nakalai Tesque, Japan) at a dose of 0 (vehicle: 0.9% saline) or 5 mg/kg body weight was administered to the animals. After the 1-week recovery period, the mice were fed the powdered diet containing DC at the concentration of 0 or 1500 ppm. To enhance hepatocellular proliferation in the liver, these mice were subjected to two-thirds partial hepatectomy (Tsuda et al., 1979) at week 3 and maintained up to week 8 to determine pre-neoplastic foci (Exp. II).

At necropsy, the mice were sacrificed at each time point (2 weeks in Exp. I and 8 weeks in Exp. II) under anesthesia with ether by exsanguination from the abdominal aorta for sampling of the liver. Tissue samples for all analyses in Exp. I and II were collected from the right lateral robe of the liver in mice. One section of each liver was fixed with natural-buffered formalin for the histochemical analysis, and another section was embedded in the OCT compound (Tissue-Tek: Miles, USA) to freeze it for evaluation of γ-glutamyltransferase (GGT) positive foci—a marker of pre-neoplastic foci—in the mice liver (Cater et al., 1985). The remaining liver samples were weighed, frozen in liquid nitrogen, and stored at −80 °C until subsequent RNA isolation and protein extraction was performed.

These experiments were carried out in accordance with the Guide for Animal Experimentation by the Tokyo University of Agriculture and Technology.

2.2. *RNA isolation and cDNA microarray analysis*

In Exp. I, a large-scale analysis of gene expression was performed using Atlas Glass Microarray Mouse 3.80 I Microarray (BD Biosciences Clontech Nippon Becton Dickinson, Japan) for spotting 3757 genes. In summary, the total RNA was isolated using TRIzol reagent, according to the manufacturer's protocol (Invitrogen, USA). The total RNA sample was pooled from 3 animals of each group, and the production of labeled cDNA probe, hybridization, and imaging data analysis for the comparison between 0 and 1500 ppm groups were performed by BD Biosciences Clontech Nippon Becton Dickinson Co. Ltd., using Atlas Image and Data Analysis Software.

Exp. II uses the two-stage hepatocarcinogenesis model. Based on the results of the gene expression analysis obtained from Exp. I, two types of pathway-specific microarrays (Mouse Stress and Toxicity PathwayFinder Gene Array and Mouse Drug

Metabolism Gene Array: GEArray; SuperArray Bioscience, USA) were performed using biotinylated cDNA with 5 μg of RNA; hybridization and chemiluminescence detection were performed using a Bio Imaging System (Lab Works 4.0: UVP, USA) according to the manufacturer's protocol. The image data obtained from GEArray were analyzed using ScanAlyze (http://rana.lbl.gov/EisenSoftware.htm). To minimize the effects of measurement variation introduced by artificial sources in analyzed data of the microarrays in Exp. I and II, genes which were up- or down-regulated at least more than 2-fold were included.

2.3. RT-PCR and real-time RT-PCR

In Exp. I, the results of the cDNA microarray were validated using the conventional reverse transcriptional polymerase chain reaction (RT-PCR) of RNA samples obtained from all the animals used in this experiment. Reverse transcription was carried out with 1 μg of RNA for cDNA synthesis using ThermoScript RT-PCR System (Invitrogen, USA) according to the manufacturer's protocol, and the cDNA aliquots were used in subsequent PCR runs with each primer set under the optimal conditions (Table 2). Band intensities obtained by electrophoresis on 2% agarose gel were analyzed using the NIH Image. Band intensities of target genes were corrected based on those of β-actin in the same cDNA sample.

In the two-stage hepatocarcinogenesis model, quantitative real-time RT-PCR with SYBR Green was performed using ABI Prism 7000 Sequence Detection System (Applied Biosystems, USA) to validate the microarray (GEArray) results. The cDNA synthesis using RNA of all the animals was performed in the same manner as Exp. I. The PCR reaction was performed according to the SYBR Green PCR master mix protocol, and it was repeated twice in triplicate for each gene. The PCR primers were designed using Primer Express software (Applied Biosystems, USA).

2.4. Histological, histochemical, and immunohistochemical evaluations

Formalin-fixed liver tissues were embedded in paraffin, sectioned, and stained with hematoxylin and eosin (H-E) for the histological examinations. Additionally, immunohistochemical staining of proliferating cell nuclear antigen (PCNA) antibody (PC10; DakoCytomation, Japan) was performed by the avidin-biotin-peroxidase complex method. The histochemical staining of GGT was performed by modifying the methods proposed by Rutenberg et al. (1969). The frozen tissues were cryosectioned and fixed using methanol. After air-drying, the freshly prepared solution containing the substrate L-glutamic acid-γ-(4-metoxy-β-naphthylamide) (Sigma–Aldrich, USA) and fast blue BBN (Wako Pure Chemical Industries, Japan) in 0.1 M Tris-buffered saline (pH 7.4) was coated onto the section. Following the incubation, the slides were transferred into a 0.1 M cupric sulfate solution. These sections were then stained with hematoxylin, and mounted in 10% glycerol. The number of PCNA-positive cells per 200–300 cells in each slide was counted from five different areas to obtain the PCNA labeling index (PCNA LI). The number of GGT-positive cells per area was calculated from the number of positive cells in all lobes on the slide and from the total area in all lobes measured using the computer-assisted image analyzer (NIH image).

2.5. Assay of activated NF-κB

Proteins were extracted from the frozen liver tissue using PRO-PREP protein extract solution (iNtRON Biotechnology, Korea). After the protein concentration measurements using the BCA Protein Assay Kit (PIERCE Biotechnology, USA), the concentrations of total and active NF-κB were determined using an enzyme immunoassay kit (Oxford Biochemical Research, USA) according to the manufacturer's protocol.

2.6. Statistical evaluation

The data were presented as the mean + S.D. Statistical analysis was performed with the statistical software (JMP 4.0.5J, SAS Institute, USA). In Exp. I, the PCR data were compared between two groups using Student's *t*-test after one-way ANOVA. In Exp. II, the data of GGT, PCNA, PCR and NF-κB were compared between two corresponding groups using Student's *t*-test after the one-way ANOVA. Additionally, Dunnett's test was used to isolate the group(s) that differed significantly from the untreated group. A *P*-value of less than 0.05 was considered to be statistically significant.

Table 1
List of genes which were observed the fluctuation$_{(>2\text{-fold})}$ on a large-scale microarray of the DC group in Exp. 1

Accession number	Classification	Gene name	Ratio (DC/Untreated)	Function (activity)
Up-regulation				
	Xenobiotic metabolism			
NM_007815		Cytochrome P450, family 2, subfamily c, polypeptide 29	4.1	Oxidoreductase, Monooxygenase
NM_009993		Cytochrome P450, family 1, subfamily a, polypeptide 2	3.6	Oxidoreductase, Monooxygenase
NM_009467		UDP-glucuronosyltransferase 2 family, member 5	2.1	Glucuronosyltransferase
NM_007817		Cytochrome P450, family 2, subfamily f, polypeptide 2	2.0	Oxidoreductase, Monooxygenase
NM_007940		Epoxide hydrolase 2, cytoplasmic	2.0	Epoxide hydrolase
NM_007621		Carbonyl reductase 2	2.0	Oxidoreductase, Carbonyl reductase
	Simple carbohydrate metabolism			
NM_008062		Glucose-6-phosphate dehydrogenase X-linked	3.0	Oxidoreductase, Glucose-6-phosphate 1-dehydrogenase
NM_008061		Glucose-6-phosphatase, catalytic	2.4	Oxidoreductase, Glucose-6-phosphate 1-dehydrogenase
	Energy metabolism			
NM_008063		Glucose-6-phosphatase, transport protein 1	2.3	Oxidoreductase, Glucose-6-phosphate 1-dehydrogenase
NM_013467		Aldehyde dehydrogenase family 1, subfamily A1	5.9	Acyltransferase, Carnitine O-palmitoyltransferase
	Simple lipid metabolism			
NM_011044		Phosphoenolpyruvate carboxykinase 1, cytosolic	2.0	Carboxy-lyase, GTP binding
NM_009948		Carnitine palmitoyltransferase 1, muscle	3.3	Acyltransferase, Carnitine O-palmitoyltransferase
NM_008097		Glutaryl-Coenzyme A dehydrogenase	2.0	Oxidoreductase, Acyl-CoA dehydrogenase, Glutaryl-CoA dehydrogenase,
	Cholesterol metabolism			
NM_015729		Acyl-Coenzyme A oxidase	2.0	Oxidoreductase, acyl-CoA oxidase
	Amino acid metabolism			
NM_019709		Site-1 protease	2.7	Serine-type endopeptidase activity
NM_007482		Arginase 1, liver	2.4	Arginase, Manganese ion binding
	Metabolism of cofactors, vitamins, and related substrates			
NM_009804		Catalase 1	2.0	Oxidoreductase, Acting on peroxide as acceptor, Peroxidase
NM_008160		Glutathione peroxidase 1	3.0	Oxidoreductase, Glutathione peroxidase

Table 1 (*Continued*)

Accession number	Classification	Gene name	Ratio (DC/Untreated)	Function (activity)
NM_007757		Coproporphyrinogen oxidase	2.1	Oxidoreductase, Coproporphyrinogen oxidase
	Other metabolism enzymes			
NM_008162		Glutathione peroxidase 4	2.0	Oxidoreductase, Glutathione peroxidase
NM_009286		Sulfotransferase, hydroxysteroid preferring 2	3.4	Alcohol sulfotransferase
NM_019946		RIKEN cDNA 1500002K10 gene	3.3	Microsomal glutathione transferase
NM_008184		Glutathione *S*-transferase, mu 6	3.2	Glutathione transferase
NM_010001		Cytochrome P450, family 2, subfamily c, polypeptide 37	3.1	Oxidoreductase, Monooxygenase
NM_010010		Cytochrome P450, 46 (cholesterol 24-hydroxylase)	2.9	Oxidoreductase, Monooxygenase
NM_009127		Stearoyl-Coenzyme A desaturase 1	2.6	Oxidoreductase, Stearoyl-CoA 9-desaturase
NM_011933		2-4-dienoyl-Coenzyme A reductase 2, peroxisomal	2.2	Oxidoreductase, peroxisome organization
NM_010240		Ferritin light chain 1	2.2	Ferric iron binding
NM_015762		Thioredoxin reductase 1	2.2	Oxidoreductase, Acting on NADH or NADPH, disulfide as acceptor, Thioredoxin-disulfide reductase
NM_007750		Cytochrome c oxidase, subunit VIIIa	2.0	Oxidoreductase, cytochrome-c oxidase
	Basic transcription factor			
NM_008712		Nitric oxide synthase 1, neuronal	2.0	Oxidoreductase, calmodulin binding, Nitric-oxide synthesis
	CDK inhibitor			
NM_010866		Myogenic differentiation 1	4.1	DNA binding, Protein binding
	Other cell adhesion protein			
NM_007670		Cyclin-dependent kinase inhibitor 2B (p15, inhibits CDK4)	2.4	Cyclin-dependent protein kinase inhibitor, Transcription factor
	Major histo-compatibility complex			
NM_010796		Macrophage galactose *N*-acetyl-galactosamine specific lectin	2.2	Sugar binding
	Extracellular transport/carrier proteins			
NM_009735		Beta-2 microglobulin	2.1	MHC class I receptor
NM_013465		Alpha-2-HS-glycoprotein	2.6	Cysteine protease inhibitor
	Oncogenes and tumor suppressors			
NM_007469		Apolipoprotein CI	2.3	Lipid transporter activity

Table 1 (*Continued*)

Accession number	Classification	Gene name	Ratio (DC/Untreated)	Function (activity)
	Trafficking/ targeting protein			
NM_008502		Lethal giant larvae homolog	2.6	Maintenance of apical/basal cell polarity
NM_008997		RAB11B, member RAS oncogene family	2.4	DNA binding, GTP binding
	Ribosomal protein			
NM_009228		Syntrophin, acidic 1	2.3	Actin binding, calmodulin binding, Protein binding
	RAN processing, turnover, and transport			
NM_009081		Ribosomal protein L28	3.5	Structural constituent of ribosome
	Chromatin protein			
NM_008774		Poly A binding protein, cytoplasmic 1	3.2	RNA binding
	Growth factors, cytokines, and chemokines			
NM_007690		Chromodomain helicase DNA binding protein 1	3.1	ATP-dependent helicase activity, Chromatin binding, Nucleic acid binding
NM_009142		Small inducible cytokine subfamily D, 1	2.7	Chemokine, Cytokine
	Intracellular transducers/ effectors/ modulators			
NM_009131		Stem cell growth factor	2.1	Growth factor, Nucleic acid binding
NM_009059		Ral guanine nucleotide dissociation stimulator,-like 2	2.5	Guanyl-nucleotide exchange factor
NM_009412		Tumor protein D52	2.1	Unknwon
	Proteosomal protein			
NM_007791		Cysteine rich protein	2.0	Protein binding, Zinc ion binding
NM_011189		Protease (prosome, macropain) 28 subunit, alpha	3.7	Unknwon
	Unclassified			
NM_011192		Proteaseome (prosome, macropain) 28 subunit, 3	3.3	Proteasome activator
NM_019749		Gamma-aminobutyric acid receptor associated protein	3.6	Microtubule binding, microtubule cytoskeleton organization and biogenesis
NM_016774		ATP synthase, H+ transporting mitochondrial F1	3.1	ATP biosynthesis, Hydrogen-exporting ATPase activity, phosphorylative and rotational mechanism
NM_019689		Dead ringer homolog 2 (*Drosophila*)	3.1	DNA binding, intracellular
NM_020287		Insulinoma-associated 2	3.1	Unknwon
NM_015755		Hormonally up-regulated Neu-associated kinase	3.0	Protein kinase, Protein amino acid phosphorylation
NM_008226		Hyperpolarization-activated, cyclic nucleotide-gated K+2	2.9	3′,5′-cAMP binding, potassium channel

Table 1 (*Continued*)

Accession number	Classification	Gene name	Ratio (DC/Untreated)	Function (activity)
NM_007448		Angiogenin related protein 2	2.7	Endonuclease, negative regulation of protein biosynthesis
NM_008075		Gamma-aminobutyric acid (GABA-A) receptor, subunit rho 1	2.6	GABA-A receptor, Ion channel, Neurotransmitter receptor activity
NM_010827		Musculin	2.6	Regulation of transcription, DNA-dependent
NM_013610		Ninjurin 1	2.6	Protein binding, tissue regeneration
NM_011097		Paired-like homeodomain transcription factor 1	2.6	Regulation of transcription, DNA-dependent
NM_011662		TYRO protein tyrosine kinase binding protein	2.6	Protein binding
NM_011912		Ventral anterior homeobox containing gene 2	2.6	Transcription factor activity
NM_008074		GABA-A receptor, subunit gamma 3	2.5	GABA-A receptor, Ion channel, Neurotransmitter receptor activity
NM_015740		General control of amino acid synthesis-like 1 (yeast)	2.5	Protein binding
NM_019917		Tissue-type vomeronasal neurons putative pheromone receptor	2.5	Receptor activity
NM_010896		Neurogenic differentiation 3	2.4	DNA binding, cell differentiation
NM_020012		Ring finger protein 14	2.4	Ubiquitin-protein ligase activity
NM_009429		Translationally regulated transcript (21 kDa)	2.4	Calcium ion binding, anti-apoptosis
NM_011918		Z-band alternatively spliced PDZ-motif protein	2.4	Protein binding
NM_008423		Potassium voltage gated channel, Shal-related family, member 1	2.3	Voltage-gated potassium channel
NM_008857		Protein kinase C, lamda	2.3	ATP binding, Diacylglycerol binding, Protein serine/threonine kinase, Transferase
NM_011862		Protein kinase C and casein kinase substrate in neurons 2	2.3	Cytoskeletal protein binding
NM_019517		Beta-site APP-cleaving enzyme 2	2.2	Aspartic-type endopeptidase,
NM_009902		Claudin 3	2.2	Structural molecule
NM_009903		Claudin 4	2.2	Structural molecule
NM_019626		Cerebellin 1 precursor protein	2.2	Extracellular space component
NM_008076		GABA-A receptor, subunit rho 2	2.2	GABA-A receptor, Ion channel, Neurotransmitter receptor activity
NM_008479		Lymphocyte-activation gene 3	2.2	Defense response
NM_009156		SelenoproteinW, muscle 1	2.2	Selenium binding
NM_010162		Exostoses (multiple) 1	2.1	Transferase (transferring glycosyl groups)
NM_010425		Forkhead box D3	2.1	DNA binding, transcription factor
NM_016705		Kinesin family member 21A	2.1	Microtubule motor activity
NM_011195		Pre T-cell antigen receptor alpha	2.1	Extracellular space
NM_019516		Galectin-related inhibitor of proliferation 1	2.0	lactose binding, induction of apoptosis by intracellular signals
NM_010286		Glucocorticoid-induced leucine zipper	2.0	Regulation of transcription, anti-apoptosis
NM_008935		Prominin	2.0	Phototransduction
NM_019974		Protease, serine, 20	2.0	Serine-type endopeptidase, proteolysis and peptidolysis

Table 1 (*Continued*)

Accession number	Classification	Gene name	Ratio (DC/Untreated)	Function (activity)
Down-regulation				
	Protein modification enzymes			
NM_007415		ADP-ribosyltransferase 1	0.1	NAD+ ADP-ribosyltransferase, Transferase (transferring glycosyl groups)
	Steroid metabolism			
NM_009293		Steroid sulfatase	0.4	Sulfuric ester hydrolase, Calcium ion binding
	Death receptor ligands			
NM_009369		Transforming growth factor, beta induced, 68 kDa	0.5	Cell adhesion
	Unclassified			
NM_010636		Kruppel-like factor 12	0.4	Regulation of transcription, DNA-dependent
NM_009746		B-cell CLL/lymphoma 7C	0.4	Subtype of BCL family
NM_019801		Open reading frame 18	0.4	Unknown
NM_009220		Spermiogenesis gene	0.4	Gametogenesis
NM_008648		Major urinary protein 4	0.5	Pheromone binding
NM_011615		Tumor necrosis factor (ligand) superfamily, member 19	0.5	DNA binding, Protein binding

3. Results

3.1. Analysis of DC-induced gene expressions in Exp. I

In histopathological examinations, slight but significant increases of the relative liver weight (113%) and very slight hypertrophy of hepatocytes were observed in the DC-group (data were not shown).

In the microarray analysis of the liver in mice treated with DC for 2 weeks, a total of 97 genes were up-regulated (88 genes) or down-regulated (9 genes) by two-folds or more in comparison to that of the untreated group. Among these, the metabolism-/oxidation-/reduction-related (32 genes) genes and the non-classified genes (44 genes) predominantly fluctuated (Table 1). To check the expressions of some genes, RT-PCR analyses of all the examined animals were performed. The results of the microarray and RT-PCR for each examined primer set are summarized in Table 2. The gene expression levels in RT-PCR were approximately similar to those in the microarray, and significant differences were predominantly observed in metabolism-/oxidation-/reduction-related genes, such as *Cyp1a1*, *Cyp1a2*, thioredoxin reductase 1 (*Txnrd1*), and aldehyde dehydrogenase family 1 subfamily A1 (*Aldh1a1*), between the untreated and the DC-alone group. In addition to these metabolism-/oxidation-/reduction-related genes, significant differences were observed between the genes such as chromodomain helicase DNA binding protein 1 (*Chd1*) and RAB11B (*Rab11b*).

3.2. Histological evaluations in Exp. II (two-stage liver carcinogenesis model)

Histopathologically, slight centrilobular hypertrophy of hepatocytes and diffuse, small necrotic foci were observed in the DC-alone group and the DMN + DC + PH groups (Fig. 2a and b). The deposition of lipofuscin was observed to be slight in the DC-alone group and moderate in the DMN + DC + PH group (Table 3). The number of GGT-positive cells was significantly increased in the DMN + DC + PH group in

Table 2
List of genes fluctuated in large-scale cDNA microarray and RT-PCR in Exp. 1

Accession number	Primer (upper: forward primer, lower: reverse primer)	Gene name (abbreviation)	Relative expression level (DC/untreated)	
			Microarray	RT-PCR
Up-regulated				
NM_013467	GACTTGAAGATTCAACATACC TCACAGCTTTGTCAACATCA	Aldehyde dehydrogenase family 1, subfamily A1 (*Aldh1a1*)	5.9	2.1[a] ± 0.29*
NM_009993	GCTACTTGTGACATGGCCTA AAGCCATTCAGTGAGGTGTC	Cytochrome P450, family 1, subfamily a, polypeptide 2 (*Cyp1a2*)	3.6	3.0 ± 0.65*
NM_016774	GAATCATGAATGTCATTGGA ACATTGTTGATTAGCTCCAT	ATP synthase, H+ transporting mitochondrial F1 (*Atp5b*)	3.1	2.0 ± 0.06
NM_007690	ACTGGCTCGCTCACTCTT AGGAAGTCAGTGTGGAGA	Chromodomain helicase DNA binding protein 1 (*Chd1*)	3.1	2.2 ± 0.29*
NM_009127	TGTTCGTTAGCACCTTCTTG GAAGGTGTGGTGGTAGTTGT	Stearoyl-Coenzyme A desaturase (*Scd1*)	2.6	1.4 ± 0.44
NM_008997	ATTACCTATTCAAAGTGGTGC CTCCACTCCGATGGTACT	RAB11B, member RAS oncogene family (*Rab11b*)	2.4	4.8 ± 0.28**
NM_015762	GGTTGCATACCTAAGAAGCTGATG CCATAGTTGCGCGAGTCTTTC	Thioredoxin reductase (*Txnrd1*)	2.2	4.3 ± 0.38**
NM_009131	TCGCCTGGCACCGCGCATTCA ACTCGCAGACGAAGTAGA	Stem cell growth factor (*Scgf*)	2.1	1.5 ± 0.12
NM_007791	CTACTTTGCTGAGGAGGTC CTTCTTGCCGTAACATGACT	Cysteine rich protein (*Csrp1*)	2.1	1.2 ± 0.08
NM_009992	AGGATGTGTCTGGTTACTTTG AGAAACATGGACATGCAAG	Cytochrome P450, family 1, subfamily a, polypeptide 1 (*Cyp1a1*)	–	18.7 ± 3.89**
Down-regulated				
NM_007415	CGATATCTTCAAGATAGAGC CTGAGATGTGTGGCAGTAGT	ADP-ribosyltransferase 1 (*Adprt1*)	0.1	0.1 ± 0.04**

–: not spotted.
[a] Mean ± S.D. (Mean of the untreated group = 1).
* $P < 0.05$ vs. untreated group (*t*-test).
** $P < 0.01$ vs. untreated group (*t*-test).

comparison to that in the untreated or the DMN + PH group (Fig. 2c and d; Fig. 3a). Increase in PCNA LI was significant in the DMN + DC + PH group as compared to that in the untreated or the DMN + PH group (Fig. 3b).

Table 3
Incidence of lipofuscin deposition in the liver of mice from Exp. II

Group	Number observed (*n*)	Lipofuscin deposition			
		No. of animals	±	+	++
Untreated	5	5	0	0	0
DC alone	5	1	1	3	0
DMN + PH	5	4	1	0	0
DMN + DC + PH	5	0	0	1	4

±: equivocal; +: slight; ++: moderate.

3.3. Gene expression analyses in the liver obtained from Exp. II

From the results of the gene expression analysis performed in Exp. I which mainly indicated the changes of gene expressions of metabolism (oxidation/reduction)-related genes, a metabolism-specific and, toxicity-, and stress-specific low-density microarray was performed to investigate the metabolism, oxidation, and reduction-related gene expressions in the liver obtained from Exp. II. These results are summarized in Table 4.

In addition to *Cyp1a1* and *Cyp1a2*, which were up-regulated in Exp. I, some of the genes relating to glutathione-*S*-transferase (GST) mu (*Gstm*) were up-regulated (>2-fold) in the DMN + DC + PH group compared to the DMN+PH group in the drug metabolism

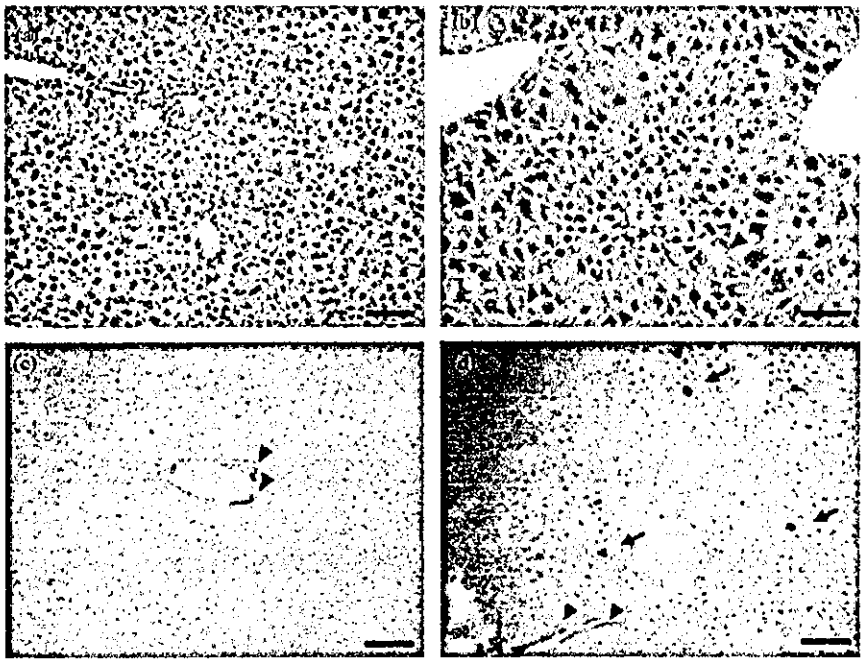

Fig. 2. Microscopic photograph of the liver in Exp. II. (a) Normal liver. Untreated group. H-E stain. Bar = 100 μm. (b) Swelling of centrilobular hepatocytes and small necrotic foci (arrow head) are observed. DMN + DC + PH group. H-E stain. Bar = 100 μm. (c) No GGT positive hepatocytes is observed. Bile duct epithelia are positive (arrow head). GGT stain. DC-alone group. 200 μm. (d) GGT positive hepatocytes (arrow) are observed. Bile duct epithelia are also positive (arrow head). GGT stain. DMN + DC + PH group. Bar = 200 μm.

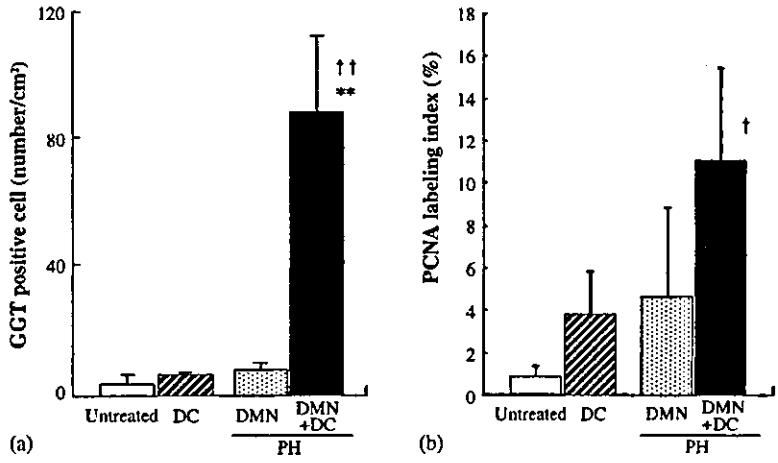

Fig. 3. Number of GGT positive cell (a) and PCNA labeling index (b) in the liver of mice from Exp. II. Columns represent the mean + S.D. of 5 animals. ** represents significant difference from the DMN + PH group at $P < 0.01$ (t-test). †,†† represent significant difference from the untreated group at $P < 0.05$ or 0.01, respectively (Dunnett's test).

Table 4
List of genes on drug metabolism fluctuated in specific microarray (Exp. II)

Accession number	Gene name	Abbreviation	Functional gene grouping[a]	Relative expression level (DMN + DC + PH/DMN + PH)
Up-regulate				
NM_009992	Cytochrome P450, family 1, sub-family a, polypeptide 1	*Cyp1a1*	P450 Gene family	15.5
NM_007940	Epoxide hydrolase 2, cytoplasmic	*Ephx2*	Epoxid Hydrolases	7.4
NM_013851	ATP-binding cassette, sub-family A (ABC1), member 8	*Abca8*	P-Glycoprotein family	6.0
NM_009993	Cytochrome P450, family 1, sub-family a, polypeptide 2	*Cyp1a2*	P450 Gene family	5.9
NM_145079	UDP glycosyltransferase 1 family, polypeptide A6	*Ugt1a6*	UDP Glycosyltransferases	5.6
NM_015751	ATP-binding cassette, sub-family E (OABP), member 1	*Abce1*	P-Glycoprotein family	3.9
NM_010358	Glutathione *S*-transferase, mu 1	*Gstm1*	Glutathione *S*-transferase	3.9
NM_008182	Glutathione *S*-transferase, alpha 2 (Yc2)	*Gsta2*	Glutathione *S*-transferase	2.9
NM_010359	Glutathione *S*-transferase, mu 3	*Gstm3*	Glutathione *S*-transferase	2.9
NM_010145	Epoxide hydrolase 1, microsomal	*Ephx1*	Epoxid Hydrolases	2.8
NM_013790	ATP-binding cassette, sub-family C (CFTR/MRP), member 5a	*Abcc5a*	P-Glycoprotein family	2.8
NM_010360	Glutathione *S*-transferase, mu 5	*Gstm5*	Glutathione *S*-transferase	2.7
NM_031884	ATP-binding cassette, sub-family G (WHITE), member 5	*Abcg5*	P-Glycoprotein family	2.7
NM_008181	Glutathione *S*-transferase, alpha 1 (Ya)	*Gsta1*	Glutathione *S*-transferase	2.5
NM_016785	Thiopurine methyltransferase	*Tpmt*	Methyltransferase	2.5
NM_010357	Glutathione *S*-transferase, alpha 4	*Gsta4*	Glutathione *S*-transferase	2.4
NM_008183	Glutathione *S*-transferase, mu 2	*Gstm2*	Glutathione *S*-transferase	2.2
NM_008184	Glutathione *S*-transferase, mu 6	*Gstm6*	Glutathione *S*-transferase	2.1
Down-regulate				
NM_011511	ATP-binding cassette, sub-family C (CFTR/MRP), member 9	*Abcc9*	P-Glycoprotein family	0.3
NM_013683	ATP-binding cassette, sub-family B (MDR/TAP), member 2	*Abcb2*	P-Glycoprotein family	0.3

[a] Grouping in Mouse Drug Metabolism Gene Array.

array. On the other hand, the down-regulation of gene expressions (<2-fold) was observed in two genes of the *p*-glycoprotein family in the metabolism array (Table 3). The oxidative and metabolic stress-related genes such as *Cyp1a1* and *Cyp1a2*, which were up-regulated in the previous microarrays, were up-regulated in the stress and toxicity array. Apart from these, glutathione reductase 1, P450 oxidoreductase (*Por*), and DNA damage-/repair-related genes such as excision repair cross-complementing rodent repair deficiency group 5 (*Ercc5*), *Pcna*, and *p53*, were also up-regulated (>2-fold). Gene expressions of cyclin D1 and growth arrest and DNA-damage-inducible 45 alpha (*Gadd45a*) were down-regulated in the stress and toxicity array (Table 5).

To check some of these gene expressions, a quantitative real-time RT-PCR was performed using samples of all mice used in Exp. II. The primers used in this PCR are summarized in Table 6. In addition to these genes, *Txnrd1*—up-regulated in Exp. I and correlated with oxidative stress, and 8-oxoguanine DNA-glycosylase 1 (*Ogg1*)—related with oxidative

Table 5
List of genes on stress and toxicity fluctuated in specific microarray (Exp. II)

Accession number	Gene name	Abbreviation	Functional gene grouping[a]	Relative expression level (DMN+DC+PH/DMN+PH)
Up-regulate				
NM_009992	Cytochrome P450, family 1, subfamily a, polypeptide 1	*Cyp1a1*	Oxidative and metabolic stress	33.1
NM_010477	Heat shock protein 1 (chaperonin)	*Hsp25*	Heating stress	18.6
NM_009831	Cyclin G1	*Ccng1*	Proliferation/carcinogenesis	11.9
NM_009993	Cytochrome P450, family 1, subfamily a, polypeptide 2	*Cyp1a2*	Oxidative and metabolic stress	8.8
NM_010481	Heat shock protein, A	*Hspa9a*	Heating stress	7.5
NM_010344	Glutathione reductase 1	*Gsr*	Oxidative and metabolic stress	6.8
NM_010442	Heme oxygenase (decycling) 1	*Hmox1*	Oxidative and metabolic stress	5.7
NM_010000	Cytochrome P450, family 2, subfamily b, polypeptide 9	*Cyp2c9*	Oxidative and metabolic stress	5.2
NM_144878	Flavin containing monooxygenase 4	*Fom4*	Oxidative and metabolic stress	5.2
NM_009998	Cytochrome P450, family 2, subfamily b, polypeptide 10	*Cyp2b10*	Oxidative and metabolic stress	4.9
NM_008303	Heat shock protein 1 (chaperonin 10)	*Hspe1*	Heating stress	4.7
NM_008898	P450 (cytochrome) oxidoreductase	*Por*	Oxidative and metabolic stress	3.9
NM_013701	Mus musculus (A-1) bilirubin/phenol UDP-glucuronosyltransferase (UGTBr/p)	*Ugt1a1*	DNA damage and repair	3.6
NM_008630	Metallothionein 2	*Mt2*	Oxidative and metabolic stress	3.2
NM_011045	Proliferating cell nuclear antigen	*Pcna*	Proliferation/carcinogenesis	3.2
NM_011729	Excision repair cross-complementing rodent repair deficiency complementation group 5	*Ercc5*	DNA damage and repair	3.1
NM_010554	Interleukin 1 alpha	*Il1a*	Inflammation	2.5
NM_011640	Transformation related protein 53	*p53*	Growth arrest/senescence	2.4
Down-regulate				
NM_007631	Cyclin D1	*Ccnd1*	Proliferation/carcinogenesis	0.4
NM_007836	Growth arrest and DNA-damage-inducible 45 alpha	*Gadd45a*	Growth arrest/senescence	0.4

[a] Grouping in mouse stress and toxicology PathwayFinder Gene Array.

stress and DNA damage were also evaluated. The expression levels in the mice liver of the DC-alone group and the DMN+DC+PH group were compared to those of the untreated group; the results are shown in Fig. 4. The up- or down-regulation of gene expressions by the DC treatment with or without DMN+PH was observed in nine genes. In particular, *Cyp1a1*, *Cyp1a2*, *Por*, and *Ogg1* were significantly up-regulated in the DC-alone group and the DMN+DC+PH group as compared to the untreated or the DMN+PH group. On the other hand, a remarkable down-regulation of gene expression by the DC treatment was observed only in *Gadd45a*. The gene expression of *p53* was contradictory to that obtained by the microarrays.

3.4. Concentration of total and activated NF-κB

From the gene expression analyses and histopathological evaluation in the liver of the mice used in Exp. II, the concentrations of activated NF-κB, which are associated with inflammation due to necrosis and are partially correlated with the oxidative stress-signaling via *Txnrd1*, were measured in all the mice. There were no consistent changes in the concentration of total NF-κB between the groups. On the other hand,

Table 6
Primers of genes used for real-time RT-PCR (Exp. II)

Accession number	Abbreviation of gene name	Primer (upper: forward primer, lower: reverse primer)
NM_009992	*Cyp1a1*	AGGATGTGTCTGGTTACTTTG
		AGAAACATGGACATGCAAG
NM_009993	*Cyp1a2*	GCTACTTGTGACATGGCCTA
		AAGCCATTCAGTGAGGTGTC
NM_008184	*Gstm6*	TTCCCAATCTGCCCTACTTGA
		TCTCCACACAGGTTGTGCTTTC
NM_008898	*Por*	GCCTGCCTGAGATCGACAAG
		GGGTCGCCTTCTCCGTATGT
NM_011729	*Ercc5*	TCAACTAGGACTGGACCGTAACAA
		AGTTGGTATCCCTTCCGTATAGTCA
NM_007836	*Gadd45a*	ACGGTCGGCGTGTACGA
		CAGGCACAGTACCACGTTATG
NM_015762	*p53*	CGCTGCTCCGATGGTGAT
		TCGGGATACAAATTTCCTTCCA
NM_015762	*Txnrd1*	GGTTGCATACCTAAGAAGCTGATG
		CCATAGTTGCGCGAGTCTTTC
NM_010957	*Ogg1*(8-oxoguanine DNA-glycosylase 1)	CAGCATAAGGTCCCCACAGATT
		GCCAACAAAGAACTGGGAAACT

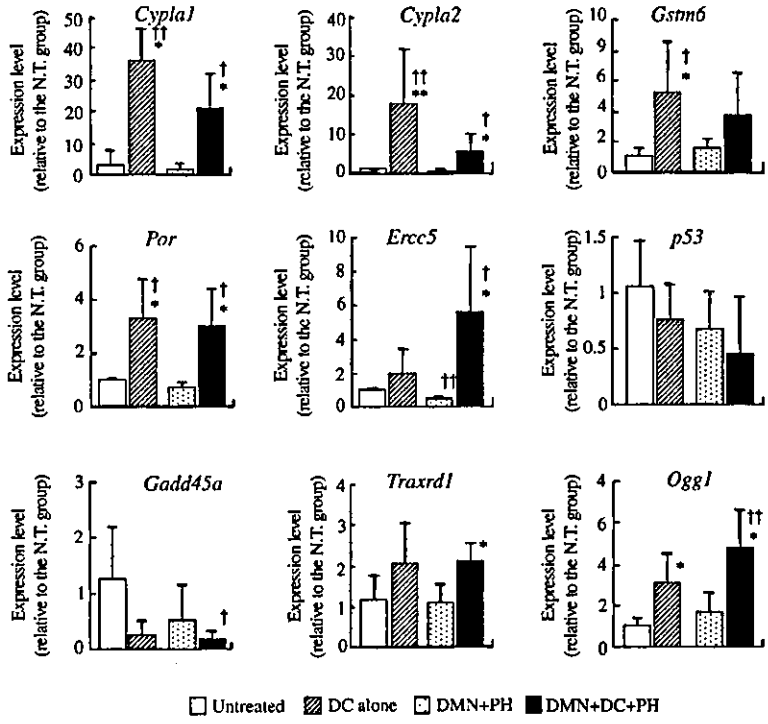

Fig. 4. Genes fluctuated in the both DC-treated groups from Exp. II. Columns represent the mean + S.D. of 5 animals. *,** represents significant difference from the DMN + PH group at $P < 0.05$ or 0.01, respectively (*t*-test). †,†† represents significant difference from the untreated group at $P < 0.05$ or 0.01, respectively (Dunnett's test).

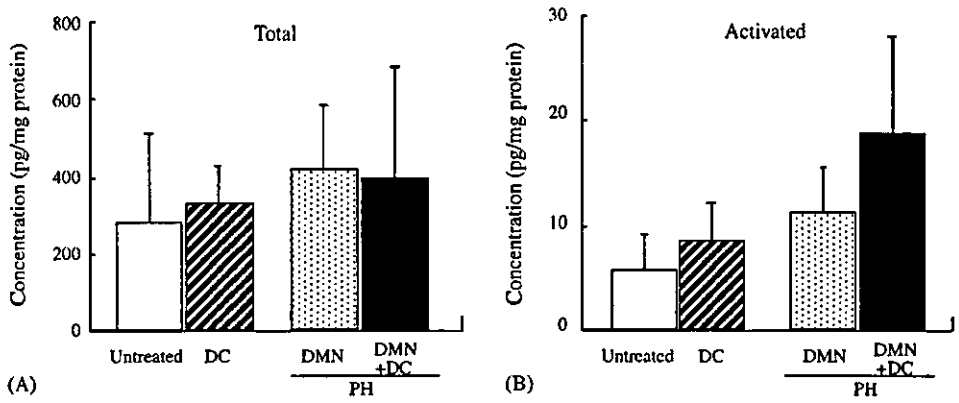

Fig. 5. Concentrations of total (A) and activated (B) NF-κB in the liver of mice from Exp. II. Columns represent the mean + S.D. of 5 animals.

a slight increase in the concentration of the activated NF-κB was observed in the DC-alone group and DMN + DC + PH groups as compared to the untreated or DMN + PH group; further, the concentration in the DMN + DC + PH group was three times higher than that in the untreated group (Fig. 5).

4. Discussion

DC has already been evaluated by the Food and Agriculture Organization (FAO)/World Health Organization (WHO) Joint Expert Committee on Food Additives (JEFCA) (WHO, 2000). In the 18-month carcinogenicity study, where mice were fed on a diet containing DC in doses of 1500, 500, 100, 10, and 0 ppm, hepatocellular adenoma was observed in the groups fed with 500 ppm or more of DC, and both hepatocellular carcinoma and adenoma were observed in the groups fed with 1500 ppm of DC (WHO, 2000). The other treatment-related histopathological finding in the liver was the hepatocellular necrosis in groups fed with 100 ppm or more of DC (WHO, 2000). Since DC shows no evidence of genotoxic effects and has a threshold, JECFA established an acceptable daily intake (ADI) of 0–7 mg/kg/day for this chemical and assumed that hepatocarcinogenesis by DC may result from the repetition of necrosis and regeneration. However, there is no supporting data for the supposed mechanism; also the exact mechanism of hepatocarcinogenesis induced in mice has not yet been clarified. With this background, this study using mice was performed to obtain mechanistic evidences for these issues.

For the large-scale gene expression analysis is performed in Exp. I, the up-regulation of the metabolism- and oxidation-/reduction-related gene expressions were predominantly observed in the liver of mice fed on a diet containing 1500 ppm of DC for 2 weeks. In particular, the gene expressions of *Cyp1a1*, *Cyp1a2*, *Aldh1a1*, and *Txnrd1* were significantly up-regulated in the DC-treated group that was subjected to the RT-PCR validation analysis. Among the CYPs, the most active for catalyzing procarcinogens is the CYP1A1 (Guengerrich and Shimada, 1991; Puntarulo and Cederbaum, 1998), and the up-regulation of CYP1A1 and/or CYP1A2 isoform(s) indirectly results in the production of very large amounts of reactive oxygen species (ROS) in comparison to other CYPs (Puntarulo and Cederbaum, 1998; Canistro et al., 2002). Thioredoxin reductase 1, *the protein of Txnrd1*, is a reduction enzyme of oxidized thioredoxin, which is a dithio-reducing enzyme induced by various oxidative stresses such as ROS and H_2O_2 (Ueno et al., 1999; Mustacich and Powis, 2000). Since those of genes were up-regulated in Exp. I, it is assumed that the treatment with a dose of 1500 ppm of DC induces the activation of metabolic pathways such as CYP1A and thioredoxin cycle and generates oxidative stress.

In Exp. II, a remarkable increase in the number of GGT positive cells was observed in the DMN + DC + PH group, and the number of PCNA positive cells increased in the DMN + DC + PH group compared to that of the untreated control group. This suggests that DC promotes the development of foci of cellular alterations in the mice liver. Additionally, small necrotic foci and the deposition of lipofuscin were ob-

served to be slight in the DC group and moderate in the DMN + DC + PH group. Lipofsucin is one of the age-associated pigments that have been regarded as cellular debris derived from lipid peroxides by the free radical-induced oxidative stress, and therefore, is considered as one of the indices of lipid peroxidation in tissues (Tsuchida et al., 1987). Our histopathological findings also support the possibility that treatment with DC at this dose results in the induction of oxidative stresses.

In the gene expression analyses of Exp. II, the up-regulation of oxidative stress-related genes, such as *Cyp1a1*, *Cyp1a2*, *Por*, *GSTs*, and *Txnrd1*, was also observed in the both of DC-treated groups. *Pro* is the gene of P450 oxidoreductase which may independently act as a co-enzyme of P450. It is generally known that some chemicals induce the production of super oxide and/or lipid peroxidation by this enzyme reaction. Therefore, the formation of lipofuscin observed in the both of DC-treated groups might result from the activation of P450 oxidoreductase via lipid peroxidation. Thioredoxin reductase 1 is a subtype of thioredoxin reductase, which utilizes NADPH to catalyze the conversion of oxidized thioredoxin to reduced thioredoxin (Luthman and Holmgren, 1982). Reduced thioredoxin provides reducing equivalents such as: (i) thioredoxin peroxidase that brakes down H_2O_2 to water; and (ii) ribonucleotide reductase that reduces ribonucleotide to deoxyribonucleotide for DNA synthesis (Laurent et al., 1964; Chae et al., 1994). Additionally, it has been reported that thioredoxin reductase plays an important role in the regulation of cell growth, inhibition of apoptosis, and inflammation closely associated with NF-κB activation (Mustacich and Powis, 2000; Sakurai et al., 2004). In fact, the concentration of activated NF-κB, an indicator of NF-κB activity that indicates the inhibition of apoptosis and an increase in inflammation and necrosis, was highest in the DMN + DC + PH group in which significant up-regulation of the *Txnrd1* expression and some necrotic foci were observed. These results may thus suggest that DC treatment inhibits apoptosis via activation of NF-κB due to the increase in thioredoxin reductase 1 and cell damages such as inflammation originating from oxidative stresses; this pathway may partially be associated with the development of GGT-positive foci.

DNA damages originating from oxidative stresses was considered as another possible pathway of hepatocarcinogenesis induced by DC, because the up- or down-regulation of DNA damage-/repair-related genes, such as *Ercc5*, *Gadd45a*, and *Ogg1*, was observed in the DMN + DC + PH group. It is known that *Ercc5*, one of nucleotide excision repair (NER) genes, is involved in the transcription-coupled repair (TCR) of DNA lesions (Cheng et al., 2000). *Gadd45a* is a p53-effector and a stress-inducible gene; it is related to the maintenance of genomic stability and the positive regulation of apoptosis (Fornace et al., 1989; Hollander et al., 1999, 2001; Smith et al., 2000; Jeffrey et al., 2002; Jin et al., 2003). In fact, the tendency of down-regulation for *p53* was observed in the DC alone and the DMN + DC + PH groups that were shown in a similar tendency of *Gadd45a*, suggesting that the instability of *p53* might be induced by treatment with DC. However, no significant differences were observed in the expression level of *p53* as well as in the levels of the activated NF-κB. These changes might be resulted to the weak levels of the gene and protein in an early tumor promotion stage of hepatocarcinogenesis, but they are considered to be enhanced as a tumor promotion stage progresses. *Ogg1* is a repaired gene of 8-hydroxy-2′-deoxyguanosine (8-OHdG); it is known as an indicator of oxidative DNA damage and is potentially involved in the carcinogenesis in various experimental models (Nakae et al., 1997; Yoshida et al., 1999; Kinoshita et al., 2002, 2003). However, it has been reported that DC was negative in the in vitro genotoxicity tests using CHO and CHL cells under the conditions of presence and absence of S9 mix (WHO, 2000). In our previous study, a single oral administration of DC did not induce DNA damages in the in vivo comet assay (Moto et al., 2003). Furthermore, remarkable fluctuations of DNA damage-/repair-related genes were not observed in the liver of the mice used in Exp. I (Table 1). These results may suggest that the assumed DNA damages originating from oxidative stresses induced by DC will not result in point mutations or chromosomal aberrations in the liver of mice fed with 1500 ppm of DC for up to 7 weeks because of the up-regulation of these DNA repair genes. However, it is unclear whether DNA damages originating from oxidative stresses will result in the occurrence of gene mutations or chromosomal aberrations due to the prolonged administration of DC. Therefore, additional studies are now in progress to clarify whether DNA damages are induced by the generation of oxidative stresses due to treatment with DC for a long period of time.

In conclusion, the present study suggests the possibility that the inhibition of apoptosis and DNA damages originating from oxidative stresses are involved in the mechanism of hepatocarcinogenesis due to DC in mice. However, further investigations comprising measurements of the 8-OHdG formation by liver DNA extraction and the production of oxidative stress-inducible substances (ROS, H_2O_2) should be performed to elucidate the relationship among DC, oxidative stresses, and DNA damages.

Acknowledgments

We are grateful to Novartis Animal Health Co. Ltd., for kindly supplying dicyclanil. This work was supported in part by a grant-in-aid for the research on safety of veterinary drug residues in food of animal origin from the Ministry of Health, Labor and Welfare of Japan (H16-shokuhin-006).

References

Afshari, C.A., Nuwaysir, E.F., Barrett, J.C., 1999. Application of complementary DNA microarray technology to carcinogen identification, toxicology, and drug safety evaluation. Cancer Res. 59, 4759–4760.

Canistro, D., Cantelli-Forti, G., Biagi, G.L., Palini, M., 2002. Re: Dioxin increases reactive oxygen production in mouse liver mitcondria. Toxicol. Appl. Pharmacol. 185, 74–75.

Cater, K.C., Gandolfi, A.J., Sipes, I.G., 1985. Characterization of dimethylnitrosamine-induced focal nodular lesions in the livers of new born mice. Toxicol. Pathol. 13, 3–9.

Chae, H.Z., Chung, S.J., Rhee, S.G., 1994. Thioredoxin-dependent peroxide reductase from yeast. J. Biol. Chem. 269, 27670–27678.

Chen, H., Liu, J., Merrick, B.A., Waalkes, M.P., 2001. Genetic events associated with arsenic-induced malignant transformation: application of cDNA microarray technology. Mol. Carcinog. 30, 79–87.

Cheng, L., Spitz, M.R., Hong, W.K., Wei, Q., 2000. Reduced expression levels of nucleotide excision repair genes in lung cancer: a case-control analysis. Carcinogenesis 21, 1527–1530.

Fornace Jr., A.J., Nebert, D.W., Hollander, M.C., Luethy, J.D., Papathanasiou, M., Frgnoli, J., Holbrook, N.J., 1989. Mammalian genes coordinately regulated by growth arrest signals and DNA-damaging agents. Mol. Cell. Biol. 9, 4196–4203.

Guengerrich, F.P., Shimada, T., 1991. Oxidation of toxic and carcinogenic chemicals by human cytochrome P450 enzymes. Chem. Res. Toxicol. 4, 391–407.

Hollander, M.C., Sheikh, M.S., Bulavin, D., Lundren, K., Augeri-Henmueller, L., Shehee, R., Molinaro, T., Kim, K., Tolosa, E., Ashwell, J.D., Rosenberg, M.D., Zhan, Q., Ferna'ndez-Salguero, P.M., Morgan, W.F., Deng, C.X., Fornace Jr., A.J., 1999. Genomic instability in Gadd45a-deficient mice. Nat. Genet. 23, 176–184.

Hollander, M.C., Kovalsky, O., Salvador, J.M., Kim, K.E., Patterson, A.D., Hairnes, D.C., Fornace Jr., A.J., 2001. DMBA carcinogenesis in Gadd45a-null mice is associated with decreased DNA repair and increased mutation frequency. Cancer Res. 61, 2487–2491.

Iida, M., Anna, C.H., Hartis, J., Bruno, M., Wetmore, B., Dubin, J.R., Sieber, S., Bennett, L., Cunningham, M.L., Paules, R.S., Tomer, K.B., Houle, C.D., Merrick, A.B., Sills, R.C., Devereux, T.R., 2003. Changes in global gene and protein expression during early mouse liver carcinogenesis induced by non-genotoxic model carcinogens oxazepam and Wyeth-14, 643. Carcinogenesis 24, 757–770.

Irwin, R.D., Boorman, G.A., Cunningham, M.L., Heinloth, A.N., Malarkey, D.E., Paules, R.S., 2004. Application of toxicogenomics to toxicology: basic concepts in the analysis of microarray data. Toxicol. Pathol. 32, 72–83.

Jeffrey, H., Dmitry, V.B., Miriam, R.A.W., Gregory, A.M., Christine, H., Lilit, V., Albert Jr., J.F., 2002. Gadd45a protects against UV irradiation-induced skin tumors, and promotes apoptosis and stress signaling via MAPK and p53. Cancer Res. 62, 7305–7315.

Jin, S., Mazzacurati, L., Zhu, X., Tong, T., Song, Y., Shujuan, S., Petrik, K.L., Rajasekaran, B., Wu, M., Zhan, Q., 2003. Gadd45a contribute to p53 stabilization in response to DNA damage. Oncogene 22, 8536–8540.

Kato, N., Shibutani, M., Takagi, H., Uneyama, C., Lee, K., Takigami, S., Mashima, K., Hirose, M., 2004. Gene expression profile in the livers of rats orally administered ethinylestradiol for 28 days using microarray technique. Toxicology 200, 179–192.

Kinoshita, A., Wanibuchi, H., Imaoka, S., Ogawa, M., Matsuda, C., Morimura, K., Funae, Y., Fukushima, S., 2002. Formation of 8-hydroxydeoxyguanosin and cell-cycle arrest in the rat liver via generation of oxidative stress by phenobarbital: association with expression profiles of $p21^{WAF1/Cip1}$, cyclin D1 and Ogg1. Carcinogenesis 24, 1389–1399.

Kinoshita, A., Wanibuchi, H., Morimura, K., Wei, M., Shen, J., Imaoka, S., Funae, Y., Fukushima, S., 2003. Phenobarbital at low dose exerts hormesis in rat hepatocarcinogenesis by reducing oxidative DNA damage, altering cell proliferation, apoptosis and gene expression. Carcinogenesis 24, 1389–1399.

Laurent, T.C., Moore, E.C., Reichard, P., 1964. Enzymatic synthesis of deoxyribonucleotides. IV. Isolation and characterization of thioredoxin, the hydrogen donor from *Escherichia coli* B. J. Biol. Chem. 239, 3436–3444.

Luthman, M., Holmgren, A., 1982. Rat liver thioredoxin and thioredoxin reductase: purification and characterization. Biochemistry 21, 6628–6633.

Moto, M., Sasaki, Y., Okamura, M., Fujita, M., Kashida, Y., Machida, N., Mitsumori, K., 2003. Absence of in vivo genotoxicity and liver initiation activity of dicyclanil. J. Toxicol. Sci. 28, 173–179.

Mustacich, D., Powis, G., 2000. Thioredoxin reductase. Biochem. J. 346, 1–8.

Nakae, D., Kobayashi, Y., Akai, H., Andoh, N., Sato, H., Ohashi, K., Tsutsumi, M., Konishi, Y., 1997. Involvement of 8-hydroxyguanine formation in the initiation of rat liver carcino-

genesis by low dose levels of *N*-nitrosodiethylanine. Cancer Res. 57, 1281–1287.

Puntarulo, S., Cederbaum, A.I., 1998. Production of reactive oxygen species by microsomes enriched in specific human cytochrome P450 enzymes. Free Radic. Biol. Med. 24, 1324–1330.

Rutenberg, A.M., Kim, H., Fischbein, J.W., Hanker, J.S., Wasserkrug, H.L., Seligman, A.M., 1969. Histochemical and ultrastructural demonstration of γ-glutamyl transpeptidase activity. J. Histochem. Cytochem. 17, 517–525.

Sakurai, A., Yasuda, K., Shoji, Y., Himeno, S., Tsujimoto, M., Kunimoto, M., Imura, N., Hara, S., 2004. Over expression of thoredoxin reductase 1 regulates NF-κB activation. J. Cell. Physiol. 198, 22–30.

Shibutani, M., Takahashi, N., Kobayashi, T., Uneyama, C., Matsutomi, N., Nishikawa, A., Hirose, M., 2002. Molecular profiling of genes up-regulating during promotion by phenobarbital treatment in a medium-term rat liver bioassay. Carcinogenesis 23, 1047–1055.

Shirai, T., 1997. A medium-term rat liver bioassay as a rapid in vivo test for carcinogenic potential: historical review of model development and summary of results from 291 test. Toxicol. Pathol. 25, 436–460.

Smith, M.L., Ford, J.M., Hollander, M.C., Bortnick, R.A., Amundson, S.A., Seo, Y.R., Deng, C.X., Hanawalt, P.C., Fornace Jr., A.J., 2000. p53-mediated DNA responses to UV radiation: studies of mouse cells lacking p53, p21, and/or gadd45 genes. Mol. Cell. Biol. 20, 3705–3714.

Tsuchida, M., Miura, T., Aibara, K., 1987. Lipofuscin and lipofuscin-like substances. Chem. Phys. Lipids 44, 297–325.

Tsuda, H., Sarma, D.S., Rajalakshmi, S., Zubroff, J., Farber, E., Batzinger, R.P., Cha, Y.N., Bueding, E., 1979. Induction of hepatic neoplastic lesions in mice with a single dose of hycanthone methanesulfonate after partial hepatectomy. Cancer Res. 39, 4491–4496.

Ueno, M., Masutani, H., Arai, J.R., Yamauchi, A., Hirota, K., Sakai, T., Inamoto, T., Yamaoka, Y., Yodoi, J., Nikaido, T., 1999. Thioredoxin-dependent redox regulation of p53-mediated p21 activation. J. Biol. Chem. 274, 35809–35815.

WHO, 2000. Toxicological evaluation of certain veterinary drug residues in food. In: 54th Meeting of the Joint FAO/WHO Expert Committee on Food Additives. WHO Food Additive Series, vol. 45, pp. 75–89.

Yoshida, M., Miyajima, K., Shiraki, K., Ando, J., Kudoh, K., Nakae, D., Takahashi, M., Maekawa, A., 1999. Hepatotoxicity and consequently increased cell proliferation are associated with flumequine hepatocarcinogenesis in mice. Cancer Lett. 141, 99–107.

2

Methacarn Fixation for Genomic DNA Analysis in Microdissected Cells

Makoto Shibutani and Chikako Uneyama

Summary

We have found methacarn, a non-crosslinking protein-precipitating fixative, to be useful for the analysis of DNA from microdissected specimens of wax-embedded tissue. In this chapter, we present the procedure regarding genomic DNA analysis in methacarn-fixed wax-embedded microdissected rat tissue. Using nested polymerase chain reaction (PCR), and a rapid extraction procedure, fragments of DNA up to 2.8 kb in size can be amplified from a 1 × 1 mm area of a 10-μm-thick tissue section. Target fragments of about 500 bp can be amplified from a single cell, but 10–20 cells are necessary for practical detection by nested PCR. Although tissue staining with hematoxylin and eosin inhibits the PCR, amplification of about 500-bp fragments is successful with 150–270 cells by single-step PCR. Immunostaining results in a substantial decrease of yield and degradation of extracted DNA. However, even after immunostaining, fragments of about 180 bp can be amplified with 150–270 cells by single-step PCR. These features demonstrate the suitability of methacarn-fixed wax-embedded tissue for practical genomic DNA analysis in terms of tissue handling, extraction efficiency, and satisfactory PCR results.

Key Words: DNA analysis; methacarn; microdissection; PCR; wax-embedded tissue.

1. Introduction

Tissue fixation and subsequent wax embedding are routinely employed for histological assessment because of the ease of handling tissues and subsequent staining as well as the good morphological preservation. Usually, formaldehyde-based fixatives are used for this purpose. However, with such crosslinking agents, there is limited performance in terms of the efficiency of extraction and quality of extracted RNA *(1–3)*, protein *(4,5)*, and genomic DNA *(6–9)*, with consequent difficulty in the analysis of microdissected, histologically defined tissue areas.

From: *Methods in Molecular Biology, vol. 293: Laser Capture Microdissection: Methods and Protocols*
Edited by: G. I. Murray and S. Curran © Humana Press Inc., Totowa, NJ

Extraction efficiency and integrity of DNA are critical for the molecular analysis of microdissected cells. Recently, we have found that methacarn, a non-crosslinking protein-precipitating fixative *(10,11)*, meets critical criteria for analysis of RNA and proteins in wax-embedded tissue sections *(5)*. In the case of DNA extraction from formalin-fixed wax-embedded tissues, the extraction protocol usually requires proteinase K treatment with extended incubation periods *(12–14)*. On the other hand, we found that methacarn fixation allows high yields and amplification of long genomic DNA segments in wax-embedded tissue sections by a simple extraction procedure *(9,15)*.

Tissue staining is essential for cellular identification in practical molecular analysis using microdissection techniques *(13,16–21)*; therefore it is important to assess the effect of tissue staining on the performance of molecular analysis *(13,17,20)*. Furthermore, analysis of gene expression or mutation in immunophenotypically defined cells would be a versatile research technique *(19)*.

In this chapter, we detail the procedures for genomic DNA analysis in methacarn-fixed wax-embedded microdissected tissue specimens *(15)*, and illustrate its suitability in terms of target fragment size and the number of microdissected cells required for DNA analysis using cresyl-violet-stained sections. We also assess the effects of tissue staining with hematoxylin and eosin (H&E) or immunohistochemical stains on subsequent analysis of genomic DNA.

2. Materials

1. Methacarn, consisting of 60% (v/v) absolute methanol, 30% chloroform, and 10% glacial acetic acid.
2. Ethanol, 99.5% (v/v).
3. Shaker for tissue agitation.
4. Xylene, reagent-grade.
5. Tissue cassettes (Tissue-Tek® Cassette series; Sakura Finetek Japan Co. Ltd., Tokyo, Japan).
6. Tissue-embedding console system (Tissue-Tek® TEC™ 5; Sakura Finetek Japan).
7. Embedding molds (Base Molds for Tissue-Tek® Embedding Rings; Sakura Finetek Japan).
8. Embedding rings (Sakura Finetek Japan).
9. Wax (Sakura Finetek Japan).
10. Microtome.
11. Hematoxylin (Tissue-Tek® Hematoxylin 3G; Sakura Finetek Japan).
12. Eosin (Tissue-Tek® Eosin; Sakura Finetek Japan).
13. 0.1% Cresyl violet solution.
14. Primary antibodies for immunohistochemistry.
15. 1% Periodic acid solution.
16. Immunostaining kit (Vectastain Elite kit; Vector Laboratories Inc., Burlingame, CA).

17. 3,3'-Diaminobenzidine, tetrahydrochloride (DAB; Dojindo Laboratories; Kumamoto, Japan).
18. Hydrogen peroxide, 30% (w/w).
19. Casein (Merck, Darmstadt, Germany).
20. Microdissector (PALM Robot-MicroBeam equipment; Carl Zeiss Co., Ltd., Tokyo, Japan).
21. Polyethylene film for microdissection, 1.35 μm thick (PALM GmbH; Wolfratshausen, Germany).
22. Nail polish.
23. TaKaRa DEXPAT™ (Takara Bio Inc., Shiga, Japan).
24. Hoechst 33258 (Molecular Probe, Eugene, OR).
25. Fluorescence spectrophotometer.
26. Thermal cycler.
27. Oligonucleotide primers.
28. PCR buffer: 20 m*M* Tris-HCl (pH 8.4), 50 m*M* KCl, 0.2 m*M* dNTP, 1.5 m*M* $MgCl_2$.
29. PLATINUM *Taq* DNA polymerase (Invitrogen Corp, Carlsbad, CA).
30. Agarose gel electrophoresis equipment.
31. Ethidium bromide (10 mg/mL; Invitrogen).
32. Agarose and DNA sequencing equipment.
33. Autoclaved ultrapure water for preparation of solutions.

3. Methods

The methods described below outline (1) the preparation of methacarn-fixed wax-embedded tissue specimens, (2) tissue staining, (3) microdissection, (4) DNA extraction from microdissected cells, and (5) polymerase chain reaction (PCR).

3.1. Preparation of Methacarn-Fixed Wax-Embedded Tissue Specimens

Methacarn solution, which is easily prepared, should be freshly made and stored at 4°C before fixation *(22)* (*see* **Note 1**).

3.1.1. Fixation and Tissue Embedding

1. Trim tissues/organs to 3 mm in thickness if possible.
2. If necessary, each tissue can be placed on a piece of filter paper or into a tissue cassette (Sakura Finetek Japan) to support tissue shape.
3. Fix tissues with methacarn for 2 h at 4°C with gentle agitation using a shaker.
4. Dehydrate tissues three times for 1 h in fresh 99.5% ethanol at 4°C with agitation.
5. Trim tissues for embedding during **step 4** if necessary.
6. Immerse tissue in xylene for 1 h and then three times for 30 min at room temperature.
7. Immerse tissues in hot wax (60°C) three successive 1-h periods.
8. Embed tissue specimens in fresh wax using a tissue-embedding console system (Sakura Finetek Japan).
9. Store wax-embedded tissue blocks at 4°C until sectioning.